Journal of Thermal Engineering
Web page info: https://jten.yildiz.edu.tr
DOI: 10.18186/thermal.977986

Research Article

Convective heat and mass transfer of chemically reacting fluids with activation energy with radiation and heat generation

P. YESODHA[1], M. BHUVANESWARI[2], S. SIVASANKARAN[3,*], K. SARAVANAN[4]

[1]*Department of Chemistry, Emerald Heights College for Women, Udhagamandalam, Tamilnadu, India*
[2]*Department of Mathematics, Kongunadu Polytechnic College, D. Gudalur, Dindigul, Tamilnadu, India*
[3]*Department of Mathematics, King Abdulaziz University, Jeddah, Saudi Arabia*
[4]*Department of Chemistry, Thiruvalluvar Government Arts College, Rasipuram, Tamilnadu, India*

ARTICLE INFO

Article history
Received: 22 September 2019
Accepted: 08 January 2020

Key words:
Heat generation; Thermal radiation; Activation energy; Chemical reaction

ABSTRACT

This study is to investigate the effect of the chemical process by activation energy on heat transference and mass transference of a fluid by heat generation parameter (Hg) and radiation parameter (Rd). Attention has been given to the changes caused on the temperature by the flow in rotating frame by the heat generation parameter, Biot number, and radiation parameter. The variation of velocity and concentration of fluid, which is chemically reacting, by the influence of the rotational parameter (β) has been incorporated. A numerical solution of the system through resulting equations has been undertaken. Effects of different flow parameters are presented by graphs and tables. Results show that activation energy increases when there is an increase in the concentration of the chemical species and that velocity decrease by the increase in porosity. With the rise of Prandtl number the temperature of the chemical system decreases. A numerical discussion on skin friction coefficients, Sherwood and Nusselt numbers has been done.

Cite this article as: Roy R, Kundu B. Convective heat and mass transfer of chemically reacting fluids with activation energy with radiation and heat generation. J Ther Eng 2021;7(5):1130–1138.

INTRODUCTION

The main objective of this current study is to evaluate the fluid flow by rotating frame in a porous medium by radiation and heat generation. This kind of flow finds great importance due to the vast application in industry and engineering fields [1–7]. The effect caused by activation energy has been studied. The smallest amount of energy required by atoms or molecules to bring about a chemical reaction is

***Corresponding author.**
*E-mail address: sd.siva@yahoo.com, sdsiva@gmail.com

This paper was recommended for publication in revised form by Regional Editor Jovana Radulovic

the activation energy. The increase in reaction rate with the increase in temperature is explained on the basis of collision theory. A certain minimum amount of energy possessed by some collisions alone results in a chemical reaction. In 1889 Svante Arrhenius initially introduced the term activation energy. Thus according to activation energy concept, the reactant molecules have to gain a certain amount of energy before they can react to yield products, and there is an energy barrier that must be crossed over by the reactants to be converted into the products. A chemical reaction will be ready to take place whenever this energy is crossed. The difference in rates of reactions is observed mainly due to the difference in activation energy because it stimulates molecules to take place in chemical reaction. Abbas et al. [8] conclude that within the boundary layer, the concentration profile is enhanced by the rising values of non-dimensional activation energy. The magnetohydrodynamic (MHD) peristaltic flow of Jeffrey matter which is chemically reactive along with activation energy was done by Hayat et al. [9]. The function of Arrhenius activation energy and the flow of MHD viscoelastic fluid with double chemical reaction were numerically computed by Mustafa et al. [10]. The mutual performance of activation energy and the double chemical reaction was scrutinized by Shafique et al. [11] in rotating fluid flow over a stretching surface. The latest field of research about activation energy can be learned in the study of Dhlamini et al. [12].

Eswaramoorthi et al. [13] investigated by the power of radiation and chemical effect, underflow on boundary layer the Soret and Dufour effects of irregular three-dimension. Sivasankaran et al. [14] analysed the consequence of slip, radiation, and chemical effect on a varied convective run of the viscous liquid in a permeable medium towards a perpendicular plate near a stagnation point. The result of nanofluid over a wedge on first order chemical effect, suction effects, and inner heat production/absorption was examined by Kasmani et al. [15]. Loganathan et al. [16] studied the appearance of radiation, chemical effect, convective heat, and cross-diffusion effects by means of Cattaneo-Christov heat up flux model to examine the changes of an Oldroyd-B fluid toward a stretching surface. The nth order chemical reaction, suction/ injection, thermal emission was examined by Makinde et al. [17] with buoyancy forces past a porous plate on uneven incompressible fluid flow. For a micropolar fluid that is enclosed by a semi-infinite permeable plate positioned vertically, Mohamed and Abo-Dahab [18] considered the special effects of chemical reaction besides thermal radiation in the occurrence of heat generation on free convection hydromagnetic heat and mass transport.

Maleque [19] initiated that for an exothermic reaction, for rising values of the pre-exposure parameter a small reduction in temperature contour is found, but for endothermic reaction opposite effects are found. By increasing the energy of activation the chemical reaction rate decreases. The extent of heat generated by a reaction can be quantified. The quantity that specifies the amount of heat is known as the "enthalpy" ΔH. When ΔH is positive the reaction is endothermic and if it is negative the reaction is exothermic. Kandasamy et al. [20] investigated alongside a wedge-shaped geometry, the collective special effects of chemical reaction and analysis of heat and mass transfer. Wahiduzzaman et al. [21] considered the impact of heat production, chemical effect, and thermal release by the flow of nanofluid on stagnation point. During the MHD flow of nanofluids, a flat plate with a chemical effect generated the radiative heat transport which was reported by Zhang et al. [22]. Natural convection heat transport alongside a perpendicular and inclined plate study by Yildiz [23] showed that local temperature values increase in distance along with the plate. Akinshilo [24] adopted the Adomain decomposition method for the heat transfer across convective straight fins taking into consideration temperature-dependent conductivity and interior generation of heat.

In the existence of chemical reaction, collective heat and mass transport have plentiful application as a geothermal reservoir, drying, dryness at the exterior of a water body, geothermal pool, aeration of permeable solids, thermal filling, cooling action in nuclear reactors, improved oil recovery, toxic waste study, wet body surface evaporation, polymer fabrication cooling, and production of ceramics. By the action of thermal energy and chemical reaction, Rana et al. [25, 26] developed above a stretching sheet the mixed and free convection flow of Casson fluid. Zeeshan et al. [27] designate the effects of viscous dissipation parameter and thermal emission for multiphase magnetic fluid above a stretching surface. Darcy-Forchheimer flow was considered by means of Rashid et al. [28] in a rotating frame, it was seen that the flow as of the extended sheet filled the porous gap and the binary chemical process was entertained.

An effort has not been made till now to study the behaviour of chemically reacting fluids with activation energy, radiation and heat generation. The authors have carried out work in this field for the major cause that this current article is to account for the outcome of radiation and heat generation of the chemically reacting fluid flow produced by rotating frame. The flow of fluid in the

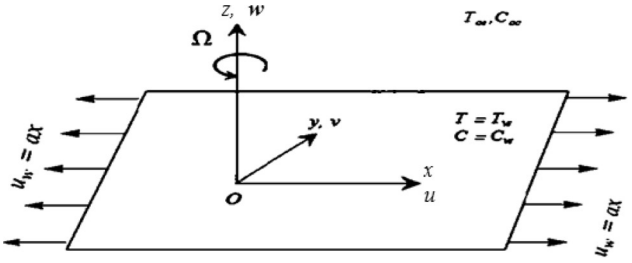

Figure 1. Schematic diagram of physical model.

rotating frame has been attracted for the reason of its extensive application in geophysics and production processes. Activation energy impact on the concentration of the fluid has also been applied.

MATHEMATICAL ANALYSIS

We are interested to analyse the rotating flow by chemical reaction in a permeable space as shown in Figure 1. Effects of activation energy and radiation have been carried out in present flow situation. A stretching level surface induces the flow which coincides with the plane $z \geq 0$. Considering the temperature T = T(x,y,z) concentration C = C(x,y,z) and velocity V =[$u(x,y,z)$, $v(x,y,z)$, $w(x, y, z)$], we get:

$$\frac{\partial u}{\partial x}+\frac{\partial v}{\partial y}+\frac{\partial w}{\partial z}=0 \tag{1}$$

$$u\frac{\partial u}{\partial x}+v\frac{\partial u}{\partial y}+w\frac{\partial u}{\partial z}-2\Omega v=\nu\frac{\partial^2 u}{\partial z^2}-\frac{\nu}{K}u-Fu^2 \tag{2}$$

$$u\frac{\partial v}{\partial x}+v\frac{\partial v}{\partial y}+w\frac{\partial v}{\partial z}+2\Omega u=\nu\frac{\partial^2 v}{\partial z^2}-\frac{\nu}{K}v-Fv^{2,} \tag{3}$$

$$u\frac{\partial T}{\partial x}+v\frac{\partial T}{\partial y}+w\frac{\partial T}{\partial z}=\alpha\frac{\partial^2 T}{\partial z^2}+\frac{Q}{\rho c_p}(T-T_\infty) -\frac{1}{\rho c_p}\frac{\partial q_r}{\partial y}, \tag{4}$$

$$u\frac{\partial C}{\partial x}+v\frac{\partial C}{\partial y}+w\frac{\partial C}{\partial z}=D\frac{\partial^2 C}{\partial z^2} -k_r^2\left(\frac{T}{T_\infty}\right)^n e^{\frac{-E_a}{kT}}\left(C-C_\infty\right), \tag{5}$$

where u, v and w are velocity components, respectively. Ω is the angular velocity, $\nu=\left(\frac{\mu}{\rho}\right)$ is kinematic viscosity, μ dynamic viscosity and ρ the density of the flowing fluid. K represents porous medium permeability and D is the solute diffusivity, k denotes thermal conductivity, c_p is at constant pressure the specific heat, $\alpha=\left(\frac{k}{\rho C_p}\right)$ is thermal diffusivity, C_b is the drag co-efficient and $F=\left(\frac{C_b}{K^{1/2}}\right)$ non-uniform inertia co-efficient. The term $k_r^2\left(\frac{T}{T_\infty}\right)^n e^{\frac{-E_a}{\kappa T}}\left(C-C_\infty\right)$ is the modified Arrhenius function, E_a is the activation energy, k_r^2 is the chemical reaction rate constant, $k = 8.61\times10^{-5}\,eV/K$ is the Boltzmann constant, n is a unitless constant exponent fitted rate constants typically lie in the range $-1 < n < 1$.

We assume that the working medium is optically thick and the thermal radiation is local. When the medium is optically thick, the radiation can be approximated as an isotropic diffusion process by using the Rosseland approximation. By the means of the Rosseland approximation, we attain the radiative heat flux $q_{r=-}\frac{4\sigma}{3k^*}\frac{\partial T^4}{\partial y}$ where σ and k* are the Stefan-Boltzman constant and the mean absorption coefficient respectively. It is understood that within the flow field the difference in temperature is too small so that T^4 can be extended in Taylor's series. Expanding T^4 about T_∞ and neglect higher order terms we locate $T \cong 4T_\infty{}^3T - 3T_\infty{}^4$

The conditions for boundary are:

$$\begin{aligned} &u = ax, v = 0, w = 0, -k\frac{\partial T}{\partial z}=h_f\left(T_w-T\right),\\ &C = C_w \ when\ z = 0\\ &u\to 0, v\to 0, C\to C_\infty, T\to T_\infty, as\ z\to\infty \end{aligned} \tag{6}$$

Here T_∞ and T_w is ambient and constant temperature, respectively. C_∞ and C_w is ambient concentration and surface concentration and a is the stretching rate (>0).

Utilising the following variables:

$$\begin{aligned} &\eta = z\sqrt{\frac{a}{\nu}},\ \mathrm{u} = axf'(\eta),\ \mathrm{v} = axg(\eta),\ \mathrm{w} = -(a\nu)^{\frac{1}{2}}f(\eta)\\ &\theta(\eta)=\frac{\mathrm{T}-\mathrm{T}_\infty}{T_w-T_\infty},\ \ \phi(\eta)=\frac{C-C_\infty}{C_w-C_\infty} \end{aligned} \tag{7}$$

Continuity Eq. (1) is automatically satisfied. In view of Eq. (7), Eqs. (2) – (6) become

$$f'''+ff''-\lambda f'+2\beta g-\left(1+F_r\right)f'^2=0 \tag{8}$$

$$g''+fg'-f'g-2\beta f'-\lambda g-F_r g^2=0 \tag{9}$$

$$\left(\frac{1}{\mathrm{Pr}}\right)\left(1+\frac{4}{3}Rd\right)\theta''+f\theta'+Hg\theta=0 \tag{10}$$

$$\varphi''+Scf\varphi'-Sc\sigma\left[1+\delta\theta\right]^t\exp\left[-\frac{E}{1+\delta\theta}\right]\varphi=0 \tag{11}$$

with boundary conditions being

$$\begin{aligned} &f=0, f'=1, g=0, \theta'=-Bi\left(1-\theta\right),\ \phi=1, at\ \eta=0\\ &f'\to 0, g\to 0, \theta\to 0, \phi\to 0\ as\ \eta\to\infty \end{aligned} \tag{12}$$

where $\beta = \frac{\Omega}{a}$ is the rotational parameter, $\lambda = \frac{\nu}{Ka}$ represents porosity parameter, $\Pr = \frac{\nu}{\alpha}$ is the Prandtl number, $Fr = \left(\frac{C_b}{K^{1/2}}\right)$ is the inertia coefficient, $Rd = \frac{4\sigma^* T_\infty^3}{kk^*}$ is the parameter for radiation, $Hg = \frac{Q}{a\rho c_p}$ is the heat generation parameter, $Sc = \frac{\nu}{D}$ is Schmidt number, $E = \frac{E_a}{\kappa T_\infty}$ is the non-dimensional activation energy, $\delta = \frac{T_w - T_\infty}{T_\infty}$ is the temperature difference parameter, $\sigma = \frac{k_r^2}{a}$ is the dimensionless reaction rate and $Bi = \frac{-h_f\sqrt{nu/a}}{k}$ is the Biot number.

The heat transfer, as a result of convection, through a fluid is given by the Nusselt number (*Nu*). The force and the mass transfer speed along the surface are defined in conditions of Sherwood number (*Sh*) and skin friction coefficient (*Cf*) as follows:

$$Nu_x = \frac{xq_w}{k(T_w - T_\infty)}, \quad Sh_x = \frac{xj_w}{D(C_w - C_\infty)}, \quad C_f = \frac{T_w}{\rho U_w^2}, \quad T_w = \mu\left(\frac{\partial u}{\partial z}\right) \tag{13}$$

$$\text{With } q_w = -k\frac{\partial T}{\partial z}|_{z=0} \ldots, j_w = -D\frac{\partial C}{\partial z}|_{z=0}. \tag{14}$$

Finally we have:

$$C_f\sqrt{Re_x} = f''(0), \frac{Nu_x}{\sqrt{Re_x}} = -\theta'(0), \frac{Sh_x}{\sqrt{Re_x}} = -\phi'(0). \tag{15}$$

Here $Re_x = \frac{ax^2}{\nu}$ show local Reynolds number

Since the leading system of equations are non-linear, to find the closed form of solutions it is not possible. Therefore, we seek a numerical solution of the governing model. With shooting technique the equations are solved by Runge-Kutta method.

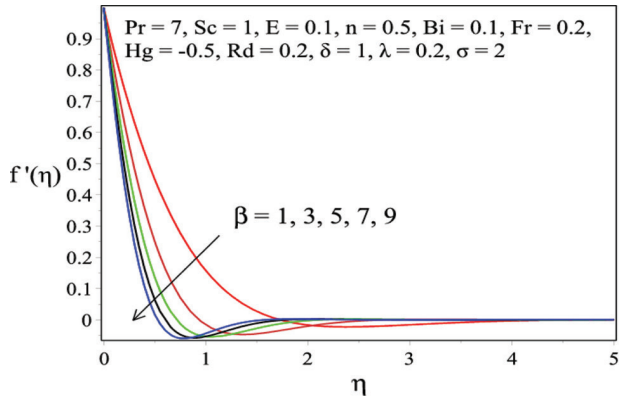

Figure 2. Velocity profiles for different values of β.

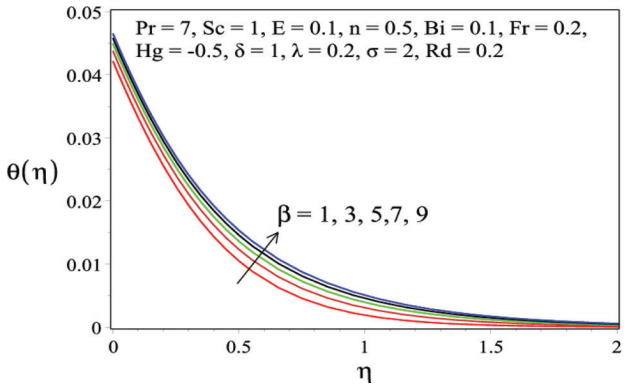

Figure 3. Temperature profiles for different values of β.

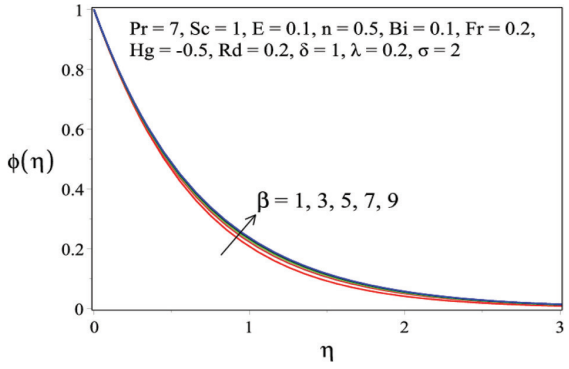

Figure 4. Concentration profiles for different values of β.

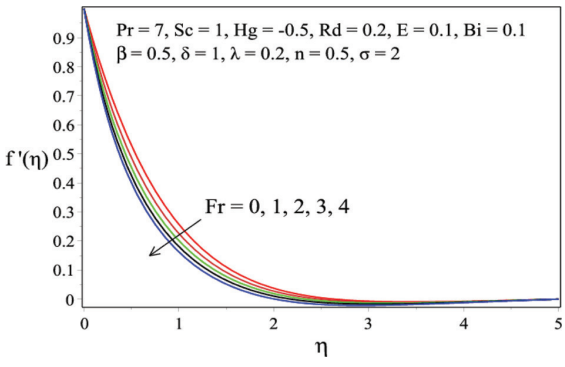

Figure 5. Velocity profiles for different values of Fr.

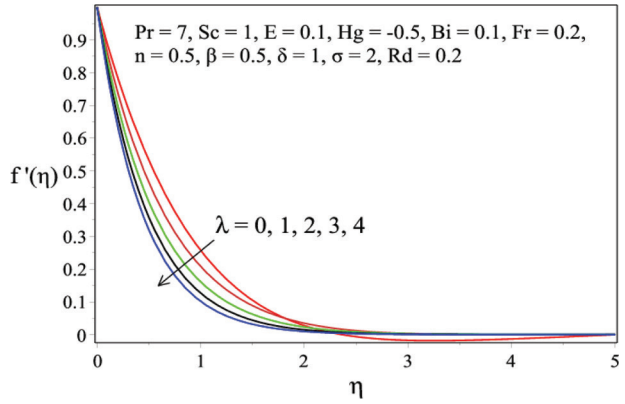

Figure 6. Velocity profiles for different values of λ.

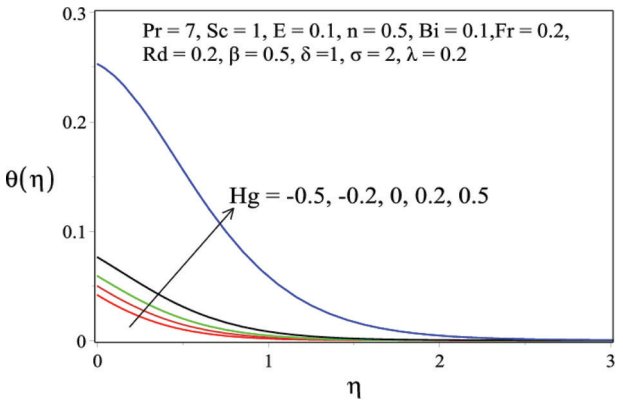

Figure 7. Temperature profiles for different values of Hg.

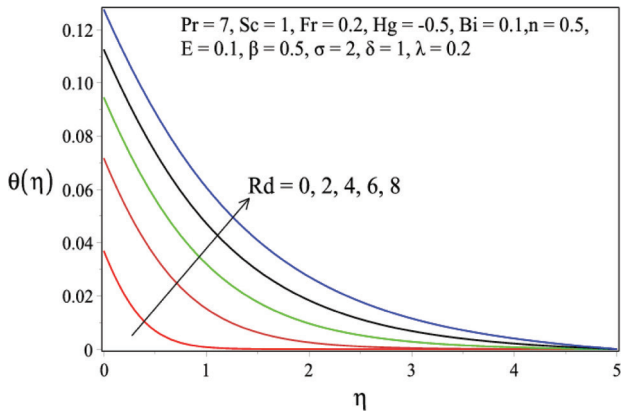

Figure 8. Temperature profiles for different values of Rd.

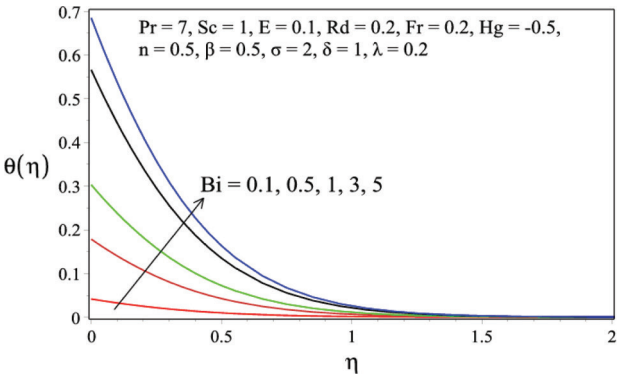

Figure 9. Temperature profiles for different values of Bi.

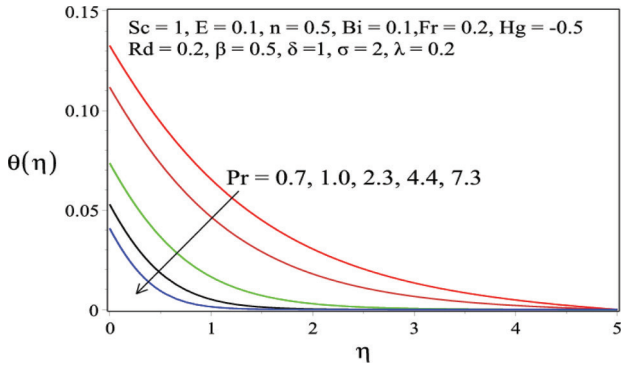

Figure 10. Temperature profiles for different values of Pr.

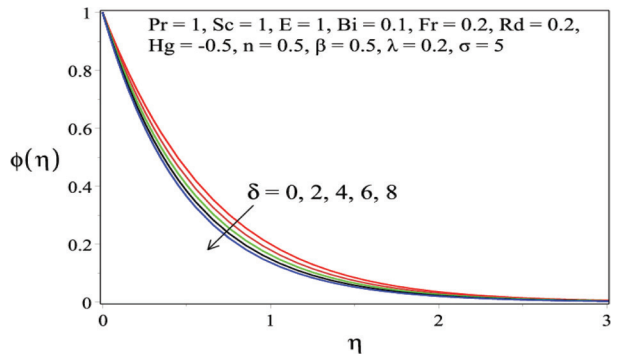

Figure 11. Concentration profiles for different values of δ.

RESULTS AND DISCUSSION

The present investigation has extended the variations of radiation parameters and heat generation parameters in the rotating framework. The impact of the rotational parameter(β), inertia coefficient (Fr), heat generation parameter (Hg), porosity parameter (λ), radiation parameter(Rd), Biot number(Bi), Prandtl number (Pr), temperature difference parameter (δ), the reaction rate (σ), the energy of activation (E), Schmidt number (Sc) and fitted rate constant (n) on velocity, temperature and concentration have been studied.

Figures 2–4 indicate the behaviour of (β) rotational parameter on velocity, concentration and temperature. Figure 2 shows that a velocity f'(η) decrease takes place for a percentage increase in rotational parameter (β). The reason for velocity decrease is that the stretching rate of the sheet reduces for larger β. In fact, when rotation in a framework

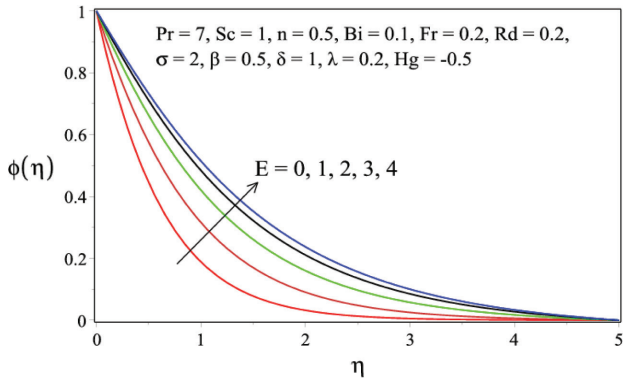

Figure 12. Concentration profiles for different values of E.

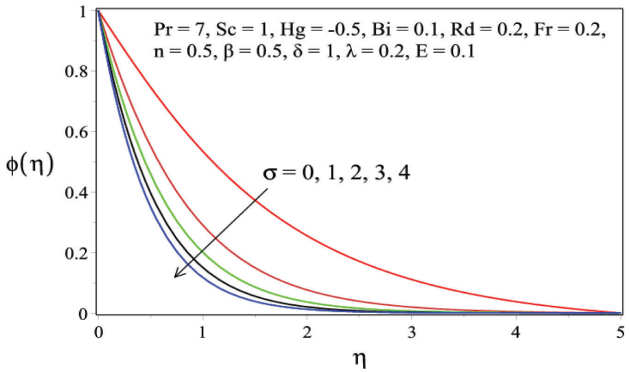

Figure 13. Concentration profiles for different values of σ.

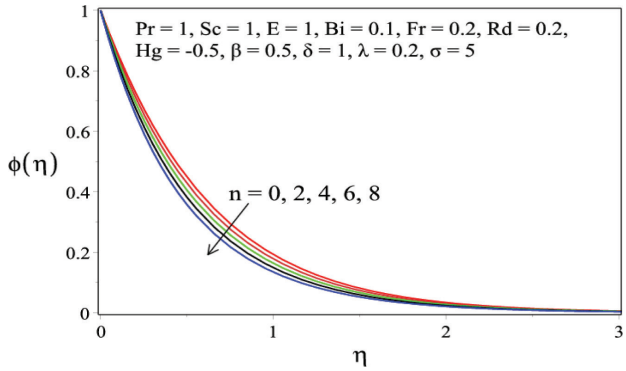

Figure 14. Concentration profiles for different values of n.

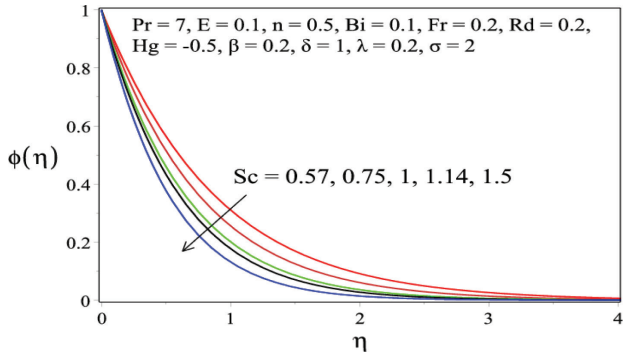

Figure 15. Concentration profiles for different values of Sc.

is increased, the stretching of the sheet will accordingly reduce and which will correspondingly slow down the flow of the fluid through it. From Figure 3, the temperature θ (η) increase with increasing β. According to Figure. 4, the concentration ϕ(η) is enhanced with increasing β. The major finding by this is that increase in porosity shows an opposite behaviour for temperature and concentration profile to the decrease in velocity. Qualitatively θ (η) and ϕ (η) through (β) show like results.

Figure 5 shows the influence of inertia coefficient (Fr) on velocity f'(η). For rising values of Fr, there is a reduction in velocity. Figure 6 indicates the effect of the porosity parameter (λ) on velocity. Similar to the actions of β, the velocity is reduced for λ value rise. When the porosity of the fluid becomes large, the flow of fluid is restricted. This is caused because the fluid becomes more viscous and thus reduces the velocity. Impacts of heat generation parameter Hg and radiation parameter Rd are illustrated in Figures 7 and 8. Biot number Bi and Prandtl number Pr are illustrated in Figures 9 and 10. Here the temperature is a rising function for the Hg, Rd, and Bi variables and decreasing function for the Pr. In Figure 7 the temperature enhances for Hg. In the same manner, it can be examined from Figure 8 that temperature increases when Rd (Rd = 0, 2, 4, 6, 8) increases. It is obvious that when heat and radiation are increased in the fluid flow in a framework the temperature shows an increasing behaviour. The power of Bi is illustrated in Figure 9 on the temperature profile. θ(η) increase by means of an increase in Bi. In Figure 10 it is found that raising the value of Pr decreases the θ(η).

From Figures11–15 it is to learn the influence of a range of parameters like activation energy, temperature difference, reaction rate, fitted rate constant, and Schmidt number on concentration. Figure 10 reveals that raising the values of δ leads to falling in ϕ(η). But from Figure 12, we understand that when activation energy (E) enhances ϕ(η) thickness also increases. In Figure 13, it is obvious that with raise in reaction rates σ values ϕ(η) come down rapidly. It can be examined from Figures 14 and 15 that ϕ(η) decreases for n and Sc increase. When n enhances, there is an increment in σ so automatically the liquid species terminate or dissolve and reduces ϕ (η). For larger Sc, mass diffusivity reduces which is in charge of the reduction in ϕ(η).

Table 1 is prepared for dissimilar porosity parameter, rotational parameter and inertia coefficient. Temperature gradient −θ' (0) and concentration gradient −ϕ'(0) is decreased by β, λ and Fr but shows an increment in velocity gradient. Table 2 highlights the force of Biot number,

Table 1. The values of $-f''(0)$, $-g''(0)$, $-\theta'(0)$, $-\phi'(0)$ for different Fr, λ, β with Pr = 7, Sc = 1, Bi = 0.1, E = 0.1, n = 0.5, σ = 2, δ = 1, Hg = –0.5 and Rd = 0.2

β	*λ*	*Fr*	*–f″(0)*	*–g″(0)*	*–θ′(0)*	*–ϕ′*(0)
		0	1.20529	0.47555	0.09584	1.48419
		1	1.44601	0.46413	0.09579	1.47866
0.5	0.2	2	1.65552	0.45789	0.09577	1.47419
		3	1.84361	0.45655	0.09574	1.47042
		4	2.01634	0.46149	0.09572	1.46708
0.5	0	0.2	1.19392	0.50949	0.09584	1.48449
	1		1.50881	0.36994	0.09578	1.47629
	2		1.79585	0.29969	0.09573	1.46891
	3		2.04949	0.25773	0.09569	1.46296
	4		2.27729	0.22936	0.09565	1.45807
1			1.41903	0.79819	0.09578	1.47475
3			1.98885	1.59609	0.09562	1.45241
5	0.2	0.2	2.43760	2.12716	0.09550	1.43977
7			2.81706	2.55234	0.09541	1.43134
9			3.15157	2.91693	0.09534	1.42517

Table 2. The values of $-\theta'(0)$, $-\phi'(0)$ for different Hg, Bi, Rd with Pr = 7, Sc = 1, β = 0.5, E = 0.1, n = 0.5, σ = 2, δ = 1, Fr = 0.2, λ = 0.2

Bi	Rd	Hg	*–θ′(0)*	*–ϕ′(0)*
0.1	0.2	–0.5	0.09583	1.48297
		–0.2	0.09501	1.48519
		0	0.09409	1.48776
		0.2	0.09237	1.49265
		0.5	0.07469	1.54241
0.1	0	–0.5	0.09630	1.48159
	2		0.09282	1.49262
	4		0.09054	1.50043
	6		0.08874	1.50665
	8		0.08724	1.51185
0.1	0.2	–0.5	0.09583	1.48297
0.5			0.41063	1.50837
1			0.69673	1.53031
3			1.30105	1.57367
5			1.57412	1.59212

Table 3. The values of $-\phi'(0)$ for different δ, σ, E, n, Pr with Sc = 1, β = 0.5, Bi = 0.1, Rd = 0.2, Hg = –0.5, Fr = 0.2, λ = 0.2

Pr	δ	E	n	σ	$-\phi'(0)$
7	1	0	0.5	2	1.54657
		1			1.04322
		2			0.76391
		3			0.62463
		4			0.56349
7	1	0.1	0.5	0	0.52394
				1	1.12026
				2	1.48297
				3	1.77032
				4	2.01621
1	1	1	0	5	1.53683
			2		1.65546
			4		1.79032
			6		1.94354
			8		2.11754
1	0	1	0.5	5	1.48519
	2				1.64085
	4				1.78078
	6				1.90685
	8				2.02100

radiation parameter and heat generation parameter on local Nusselt and Sherwood numbers. Table 3 indicates power of Prandtl number, temperature difference parameter, activation energy, rate of reaction and fitted rate constant on concentration gradient $-\phi'(0)$. It is seen that there is an increment by δ, σ, n on concentration gradient $-\phi'(0)$.

CONCLUSION

The rotating flow in a permeable space in the presence of chemical reaction and effects of activation energy and thermal radiation has been carried out in the present flow situation. The modelled equations are solved numerically. In the present analysis, the result of relevant parameters on temperature, concentration, and velocity have been described and displayed by graphs. The major points of the current study are mentioned below:

- Velocity reduces but concentration and temperature enhance for elevated values of the rotational parameter (β).
- Coefficient of inertia (Fr) and porosity parameter (λ) cause decay in velocity.
- Behaviour of heat generation parameter (Hg), radiation parameter (Rd), and Biot number (Bi) are opposite on temperature to that of Prandtl number (Pr).
- The concentration field shows a decrease with a rise in Schmidt number (Sc), temperature difference

parameter (δ), fitted rate constant (n), and reaction rate (σ).

- With the increase in concentration, the activation energy increases.
- The values λ and Fr show decrease in temperature gradient and concentration gradient.
- Bi, Rd and Hg have similar results for concentration but in temperature gradient Bi is different from Rd and Hg.

AUTHORSHIP CONTRIBUTIONS

Concept: SS, MB; Design: MB, PY; Supervision: SS, KS; Data: MB, PY; Analysis: MB, PY; Literature search: PY; Writing: PY, MB; Critical revision: SS, KS.

DATA AVAILABILITY STATEMENT

No new data were created in this study. The published publication includes all graphics collected or developed during the study.

CONFLICT OF INTEREST

The author declared no potential conflicts of interest with respect to the research, authorship, and/or publication of this article.

ETHICS

There are no ethical issues with the publication of this manuscript.

REFERENCES

[1] Turan O. Numerical investigation of laminar mixed convection in a square cross-sectioned cylindrical annular enclosure. Journal of Thermal Engineering. 2020; 6(1): 1–15.

[2] Bayareh M.B, Nourbakhsh A. Numerical simulation and analysis of heat transfer for different geometries of corrugated tubes in a double pipe heat exchanger. Journal of Thermal Engineering. 2019; 5(4): 293–301.

[3] Sheremet M.A. Bondareva N. Numerical simulation of natural convection melting in 2d and 3D enclosures. Journal of Thermal Engineering. 2019; 5(1): 51–61.

[4] Almakki M, Mondal H, Sibanda P. Entropy Generation in MHD flow of viscoelastic nanofluids with homogeneous-heterogeneous reaction, partial slip and nonlinear thermal radiation. Journal of Thermal Engineering. 2020; 6(3): 327–345.

[5] Zahmatkesh I, Ardekani R.A. Effect of magnetic field orientation on nanofluid free convection in a porous cavity: A heat visualization study. Journal of Thermal Engineering. 2020; 6(1): 170–186.

[6] Akinshilo A., Ilegbusi A.O. Investigation of Lorentz force effect on steady nanofluid flow and heat transfer through parallel plates. Journal of Thermal Engineering. 2019; 5(5): 482–497.

[7] Kaya H, Ekiciler R, Arslan K. CFD analysis of laminar forced convective heat transfer for TiO2/ Water nanofluid in a semi-circular cross-sectioned micro-channel. Journal of Thermal Engineering. 2019; 5(3): 123–137.

[8] Abbas Z, Sheikh M, Motsa S.S. Numerical solution of binary chemical reaction on stagnation point flow of Casson fluid over a stretching/shrinking sheet with thermal radiation. Energy. 2016; 95: 12–20.

[9] Hayat T, Khan A.A, Farhat Bibi, Farooq S. Activation energy and non-Darcy resistance in magneto peristalsis of Jeffrey material. Journal of Physics and Chemistry of Solids. 2019; 129: 155–161.

[10] Mustafa M, Mushtaq A, Hayat T, Alsaedi A. Numerical study of MHD viscoelastic fluid flow with binary chemical reaction and Arrhenius activation energy. International Journal of Chemical Reaction Engineering. 2017; 15(1): 127–135.

[11] Shafique Z, Mustafa M, Mushtaq A. Boundary layer flow of Maxwell fluid in rotating frame with binary chemical reaction and activation energy. Results in Physics. 2016; 6: 627–33.

[12] Dhlamini M, Kameswaran P.K, Sibanda P, Motsa S, Mondal H. Activation energy and binary chemical reaction effects in mixed convective nanofluid flow with convective boundary conditions. Journal of Computational Design and Engineering. 2019; 6: 149–158.

[13] Eswaramoorthi S, Bhuvaneswari M, Sivasankaran S, Rajan S. Soret and Dufour effects on viscoelastic boundary layer flow over a stretching surface with convective boundary condition with radiation and chemical reaction, Scientia Iranica B. Mech. Engg. 2016; 23(6): 2575–2586.

[14] Sivasankaran S, Niranjan H, Bhuvaneswari M. Chemical reaction, radiation and slip effects on MHD mixed convection stagnation-point flow in a porous medium with convective boundary condition. International Journal of Numerical Methods for Heat & Fluid Flow. 2017; 27(2): 454–470.

[15] Kasmani R.M, Sivasankaran S, Bhuvaneswari M., Siri Z. Effect of chemical reaction on convective heat transfer of boundary layer flow in nanofluid over a wedge with heat generation/absorption and suction. Journal of Applied Fluid Mechanics. 2016; 9: 379–388.

[16] Loganathan K, Sivasankaran S, Bhuvaneswari M, Rajan S. Second-order slip, cross-diffusion and chemical reaction effects on magneto-convection

of Oldroyd-B liquid using Cattaneo-Christov heat flux with convective heating. Journal of Thermal Analysis and Calorimetry. 2019; 136: 401–409.

[17] Makinde O.D, Olanrewaju P.O, Charles W.M. Unsteady convection with chemical reaction and radiative heat transfer past a flat porous plate moving through a binary mixture, Afrika Matematika, 2011; 22: 65–78.

[18] Mohamed R.A, Abo-Dahab S.M. Influence of chemical reaction and thermal radiation on the heat and mass transfer in MHD micropolar flow over a vertical moving porous plate in a porous medium with heat generation. International Journal of Thermal Sciences. 2009; 48: 1800–1813.

[19] Maleque K.A. Effects of binary chemical reaction and activation energy on MHD boundary layer heat and mass transfer flow with viscous dissipation and heat generation/absorption. Thermodynamics. 2013; article ID: 284637, 1–9.

[20] Kandasamy R, Periasamy K, Prabhu K.K.S. Effects of chemical reaction, heat and mass transfer along a wedge with heat source and concentration in the presence of suction or injection, International Journal of Heat and Mass Transfer. 2005; 48: 1388–1394.

[21] Wahiduzzaman M, Khan M.S, Karim I. MHD convective stagnation flow of nanofluid over a shrinking surface with thermal radiation, heat generation and chemical reaction, Procedia Engineering, 2015; 105: 398–405.

[22] Zhang C, Zheng L, Zhang X, Chen G. MHD flow and radiation heat transfer of nanofluids in porous media with variable surface heat flux and chemical reaction. Applied Mathematical Modelling. 2015; 39: 165–181.

[23] Yildiz S. Investigation of natural convection heat transfer at constant heat flux along a vertical and inclined plate, Journal of Thermal Engineering, 2018; 4(6): 2432–2444.

[24] Akinshilo A.T. Analytical decomposition solutions for heat transfer on straight fins with temperature dependent thermal conductivity and internal heat generation. Journal of Thermal Engineering. 2019; 5(1): 79–92.

[25] Rana S, Mehmood R, Akbar N.S. Mixed convective oblique flow of a Casson fluid with partial slip, internal heating and homogeneous–heterogeneous reactions. Journal of Molecular Liquids. 2016a; 222: 1010–1019.

[26] Rana S, Mehmood R, Narayana P, Akbar N. Free convective non-aligned non-Newtonian flow with non-linear thermal radiation. Communications in Theoretical Physics. 2016b; 66(6): 687–693.

[27] Zeeshan A, Majeed A, Fetecau C, Muhammad S. Effects on heat transfer of multiphase magnetic fluid due to circular magnetic field over a stretching surface with heat source/sink and thermal radiation. Results in Physics. 2017; 7: 3353–3360.

[28] Rashid S, Hayat T, Qayyum S, Ayub M, Alsaedi A. Three-dimensional rotating Darcy-Forchheimer flow with activation energy. International Journal of Numerical Methods for Heat & Fluid Flow. 2019; 29(3): 935–948.